A DNA vaccine strategy to activate natural killer cells for therapeutic targeting of XPO1-positive tumors

Pauline Rettman[1†], Matthew D. Blunt[1†], Berenice Mbiribindi[1‡], Rebecca Fulton[1], Ralf B. Schittenhelm[2], Andres Vallejo Pulido[1], Leidy Bastidas-Legarda[1], Marta E. Polak[1], Rochelle Ayala[3], Anthony W. Purcell[3], Aymen Al-Shamkhani[4], Christelle Retiere[5], Salim I. Khakoo[1*].

[1]School of Clinical and Experimental Sciences, Faculty of Medicine, University of Southampton, Southampton, UK

[2]Monash Biomedical Proteomics & Metabolomics Facility, Biomedicine Discovery Institute and Department of Biochemistry and Molecular Biology, Monash University, Clayton, Victoria, Australia

[3]Biomedicine Discovery Institute and Department of Biochemistry and Molecular Biology, Monash University, Clayton, Victoria, Australia

[4]School of Cancer Sciences, Faculty of Medicine, University of Southampton, Southampton, UK

[5]Etablissement Français du Sang, 44011 Nantes Cedex 01, France

[†] These authors contributed equally to this work

[‡]Current address: Department of Surgery/Transplant Division, Stanford University School of Medicine, 1201 Welch Road, MSLS P328, Stanford, CA 94305-5492

* To whom correspondence should be addressed:

Salim I. Khakoo
Faculty of Medicine
University of Southampton
Henry Wellcome Laboratories
Level E, South Academic Block
Southampton General Hospital
Tremona Road
Southampton
SO16 6YD
Tel: 023 8120 4004
s.i.khakoo@soton.ac.uk

Conflict of interest: University of Southampton (SIK, MDB, PR and RF) have a patent application pending for peptide-based immunotherapy. All other authors declared that no conflict of interests exist.

Abstract

Natural killer (NK) cells are increasingly being recognized as agents for cancer immunotherapy. KIR2DS2 is an activating killer-cell immunoglobulin-like receptor (KIR) expressed by NK cells, which has been associated with protective responses to cancer and viral infections. KIR2DS2 binds conserved viral peptides in the context of MHC class I, but to date no cancer-associated peptide ligands that bind activating KIR have been described.

In order to determine if targeting KIR was a feasible strategy for mobilizing anti-cancer immune responses we established a peptide-based KIR targeting DNA vaccine. Immunizing KIR-Tg mice with the vaccine construct generated *in vivo* peptide-specific activation of KIR2DS2-positive NK cells leading to canonical and cross-reactive peptide specific immune responses *in vitro*. Using immunopeptidomics we identified the nuclear export protein XPO1, which has been associated with poor prognosis in multiple cancers, as providing an HLA-C restricted cancer-associated peptide ligand for KIR2DS2-positive NK cells. DNA vaccination of KIR-Tg mice led to both peptide specific and non-specific tumor cell killing, and protective anti-cancer responses *in vivo*. We thus show the feasibility of targeting KIR as a strategy that activates NK cells to generate *in vivo* anti-cancer immune responses, and identify XPO1 as a novel target for NK cells.

Introduction

The potential of natural killer (NK) cells for treating cancer is now becoming recognized (1). However defining the role of NK cells in a personalized medicine strategy to treat cancer requires detailed understanding of the receptor:ligand interactions between NK cells and their cancer targets (2, 3). One important family of NK cell receptors are the killer cell immunoglobulins like receptors (KIR). These form a polymorphic gene family of receptors with MHC class I ligands (4). KIR have been implicated in susceptibility to and the outcome of many different cancers (5-11) Thus targeting the KIR has the potential to form part of a therapeutic strategy to treat cancer (12).

The KIR can be activating or inhibitory with the MHC class I ligand specificities of the inhibitory KIR being relatively well defined. However the ligand specificities of the activating KIR have been much harder to identify. Recent work has shown that activating KIR can have an MHC class I-restricted peptide specificity (13-16). Whilst T cell receptors have a tight restriction on the peptide:MHC complexes that they bind, the KIR recognize families of peptide:MHC complexes with the inhibitory KIR recognizing HLA molecules in a broad motif-based manner allowing recognition of multiple HLA class I allotypes (17, 18). KIR2DS2 is an activating receptor that recognizes group 1 HLA-C molecules, in combination with different viral and synthetic peptides and we have recently shown that KIR2DS2 recognizes highly conserved flaviviruses and hepatitis C peptides with an alanine-threonine sequence at the C-terminal -1 and -2 positions of the peptide in the context of HLA-C (14, 19).

To date no cancer-associated peptides that bind activating KIR have been identified. This is relevant as activating KIR have been associated with protective responses against cancer. KIR

haplotypes containing activating KIR confer protection against relapse of acute myeloid leukemia (AML) following bone marrow transplantation, and this has been mapped to the region of the KIR locus that contains KIR2DS2 (20-22). In cord blood transplantation this benefit is accentuated if the recipient of the transplant has group 1 HLA-C allotypes, the putative ligands for KIR2DS2 (23). KIR2DS2 has also been associated with protection against a number of solid tumors including cervical neoplasia, breast cancer, lung cancer, colorectal cancer and hepatocellular carcinoma (6, 7, 24-26). *In vitro*, recognition of cancer cell lines for KIR2DS2 has been observed, but is not specific and also encompasses inhibitory KIR2DL2/3 (27). Additionally, KIR2DS2-positive NK cells appear to express higher levels of FcγRIII (CD16), have enhanced functionality *in vitro* as compared to their KIR2DS2-negative counterparts and confer enhanced protection against glioblastoma in a xenograft model (28). Consistent with this enhanced functionality, in a clinical trial of an anti-GD2 antibody in neuroblastoma, KIR2DS2-positive patients had improved survival compared to KIR2DS2-negative patients (29). Taken together these studies suggest that KIR2DS2 has potential as a target for anti-cancer therapies.

Currently NK cell immunotherapeutics are based upon adoptive therapies, CAR-NK cells, cytokines, bi- and tri-specific killer cell engagers and checkpoint blockade (30-33). However as KIR have peptide:MHC specificity there is potential for developing peptide-based approaches to activate NK cells in a manner analogous to targeting cytotoxic T cells (34). This has additional benefit as a single KIR has a broad peptide:MHC class I specificity and so has the potential to recognize multiple different peptide:MHC combinations. We therefore sought to investigate the potential for targeting KIR in a peptide specific manner.

Results

Activation of NK cells using a peptide:MHC based vaccine strategy

To target KIR2DS2 as a cancer immunotherapy we developed a peptide:MHC (pMHC) DNA construct that expressed HLA-C*0102 linked to peptides separated by a T2A self-cleaving sequence. Two previously described KIR2DS2-binding peptides were used for this: LNPSVAATL (C*0102-LNP) and IVDLMCHATF (C*0102-IVDL) (14). The constructs were used as naked DNA vaccines to immunize KIR transgenic (KIR-Tg) mice (35). These mice express a human KIR haplotype B locus including KIR2DS2 and are backcrossed onto an MHC class I negative background. KIR-Tg mice were injected intramuscularly with 50µg of DNA, without additional adjuvant, weekly for two weeks. Mice were sacrificed one week after the final injection, and splenocytes and hepatic lymphocytes isolated. Results were compared to DNA constructs encoding HLA-C*0102 alone, or DNA encoding HLA-C*0102 in combination with a control peptide, IVDLMCHAAA (C*0102-AAA), in which the P9 and P10 residues of the peptide IVDLMCHATF had been mutated to alanine to abrogate binding to KIR2DS2 and HLA-C*0102 respectively. Injection with DNA encoding viral peptides induced activation of splenic NK cells as indicated by KLRG1 expression for both constructs, but of hepatic NK cells only by C*0102-IVDL (Figure 1A and Supplemental Figure 1). KLRG1 expression was upregulated to a significantly greater extent on KIR2DS2-positive (KIR2DS2+) versus KIR2DS2-negative (KIR2DS2-) splenic NK cells ($p<0.01$ for C*0102-IVDL and $p<0.05$ for C*0102-LNP), but not by control constructs (Figure 1B). Activation was most marked in mice injected with C*0102-IVDL compared to C*0102-LNP, consistent with the stronger *in vitro* binding previously noted (14). Furthermore, activation of hepatic NK cells was noted only with the C*0102-IVDL construct, with the expression of KLRG1 being higher on the KIR2DS2-positive population ($p<0.01$) (Figure 1C). KLRG1 was upregulated on both mature CD11b+CD27+ and terminally mature CD11b+CD27- splenic NK

cells by C*0102-IVDL, and specific activation of KIR2DS2+ NK cells was most marked on the CD11b+CD27+ splenocytes, as compared to terminally differentiated CD11b+CD27- NK cells (Figures 1D-G). Similarly after four weekly injections we observed activation of NK cells, with upregulation of KLRG1 on splenic and hepatic NK cells with both peptide-containing constructs, and KIR2DS2-specific activation in the CD11b+CD27+ double-positive population with C*0102-IVDL (Supplemental Figure 2).

KIR2DS2+ and KIR2DS2- splenic NK cells from mice vaccinated with C*0102-IVDL and C*0102-AAA were profiled by RNA seq (Supplemental Figure 3 for gating strategy). Principal component analysis (PCA) showed specific responses in KIR2DS2+ NK cells which separated into 2 distinct clusters based on vaccine type, in contrast to the KIR2DS2- NK cells (Figure 2A). Those mice receiving C*0102-IVDL had upregulation of genes in pathways associated with cellular metabolism, as compared to those receiving control C*0102-AAA vaccination (Figure 2B). Differential gene expression analysis identified 54 differentially expressed genes (FDR<0.05) between the KIR2DS2+ NK cells from the C*0102-IVDL versus control groups (Supplemental Table 1). These included upregulation in genes associated with: RNA binding and splicing; metabolism, especially glutathione metabolism; and regulation of IFN alpha (Figure 2C). Comparing KIR2DS2+ NK cells from the C*0102-IVDL group with KIR2DS2+ NK cells from the control group we observed downregulation of genes related with histone H3 dimethylation at K4 (H3K4me2) and trimethylation at K27 (H3K27me3), consistent with a change in transcriptional regulation induced by vaccination (Supplemental Figure 4).

To test *in vivo* activity of the DNA vaccination strategy, KIR-Tg mice were inoculated subcutaneously in the flank with B16F10 melanoma cells and injected intramuscularly with

DNA on the same day and one week later. Growth of B16F10 cells was significantly attenuated by day 12 in mice given C*0102-IVDL as compared to those given C*0102-AAA or unvaccinated ($p<0.001$) (Figure 2D). In vitro, KIR2DS2+ NK cells from C*0102-IVDL-vaccinated mice had increased degranulation to B16F10 cells as compared to the control vaccinated mice ($p<0.05$) (Figure 2E). As B16F10 cells do not express HLA-C these data indicate that DNA vaccination with C*0102-IVDL can induce MHC class I unrestricted anti-tumor responses. Therefore, to identify peptide-specific NK cell responses, NK cells were tested against the MHC class I-negative target human cell line 721.221 transfected with either HLA-C or HLA-C in combination with the peptides LNPSVAATL and IVDLMCHATF (14). KIR2DS2+ NK cells from mice vaccinated with the IVDLMCHATF demonstrated increased activity against 721.221 cells expressing HLA-C*0102 in combination with KIR2DS2-binding peptides as compared to 721.221 cells transfected with HLA-C*0102 alone (Figure 2F). These data establish proof-of-concept for a peptide based approach to activate NK cells through KIR2DS2 and to recognize target cells in peptide dependent and independent manners.

KIR2DS2 recognizes a cancer associated antigen

To investigate the potential use of an NK cell vaccine in a cancer strategy we selected hepatocellular carcinoma (HCC) as being a clinically important target. It is the second commonest cause of cancer-related mortality, lacks chemotherapeutic treatment options and, in an immunogenetic study KIR2DS2 in combination with HLA-C group 1 has been shown to confer a clinical benefit following HCC resection (7, 36). The hepatocellular carcinoma cell line Huh7 was used to identify cancer-associated KIR2DS2-binding peptides. This cell line expresses HLA-C at undetectable levels on the cell surface and so it was transfected with the known KIR2DS2 ligand HLA-C*0102 (37). We sequenced MHC class I bound peptides from Huh7 cells transfected with HLA-C*0102 (Huh7:C*0102) and from parental Huh7 cells

following elution with the pan class I antibody W6.32. We identified ~5800 and ~7200 peptides from Huh7 and Huh7:C*0102 cells respectively (Supplemental Table 2). The Huh7 immunopeptidome consisted mainly of peptides carrying a C-terminal lysine or arginine residue which is characteristic of the HLA-A*11 binding motif (Figure 3A). In contrast, epitopes identified from the Huh7:C*0102 cell line contained two distinct populations, one with the HLA-A*11 binding motif and one with an HLA-C*0102 binding motif. From this comprehensive repertoire of HLA class I binders, only one peptide, NAPLVHATL, was identified that conformed to both the HLA-C*0102-binding motif (xxPxxxxxL) and the KIR2DS2-binding motif (xxxxxxATx). NAPLVHATL, which was identified by three independent, high-quality peptide-spectrum matches (Figure 3B), is derived from the nuclear export protein exportin-1 (XPO1). This protein is upregulated in many hematological malignancies and solid tumors including HCC, is generally associated with a poor prognosis in cancer and has been successfully targeted in clinical trials of refractory multiple myeloma (38-43).

Data-independent acquisition mass spectrometry (DIA-MS) was used to quantify epitopes between the transfected Huh7:C*0102 and the parental Huh7 cell line (Supplemental Table S]3). The peptide NAPLVHATL was eluted at 15 fold greater levels in Huh7:C*0102 compared to Huh7 cells, consistent with it being presented by HLA-C*0102. Searching of the IEDB database revealed that this peptide has been previously eluted from C1R and 721.221 B-lymphoblastoid cell lines transfected with HLA-C*0102 (44, 45). In vitro, NAPLVHATL bound HLA-C*0102 expressed by TAP-deficient 721.174 cells to a similar level as VAPWNSFAL, a previously defined HLA-C*0102 binding peptide (46), and at saturating concentrations bound a KIR2DS2 tetramer (Figures 3C, D and Supplemental Figure 5).

KIR2DS2+/KIR2DL2/3- primary NK cells upregulated CD107a expression following incubation with 721.221 cells expressing NAPLVHATL in combination with HLA-C*0102 to a greater extent than other NK cell subsets (Figure 3E and Supplemental Figure 6). The KIR-negative NKL cell line was transfected with KIR2DS2 (NKL-2DS2) or with KIR2DL2 (NKL-2DL2) and incubated with the 721.221 cells expressing HLA-C*0102 with or without NAPLVHATL. NKL-2DS2, but not NKL-2DL2 demonstrated enhanced VAV1 phosphorylation in the presence of NAPLVHATL (Figure 3F). Thus, NAPLVHATL is recognized by KIR2DS2 in the context of HLA-C*0102, and this interaction activates NK cells.

To test the role of endogenously expressed XPO1 in KIR2DS2-mediated recognition, XPO1 was knocked down in Huh7:C*0102 cells using siRNA (Figure 4A). NKL-2DS2 cells, but not NKL-2DL2, killed XPO1 knockdown Huh7:C*0102 cells less efficiently than those transfected with control siRNA at all effector:target (E:T) ratios tested ($p<0.001$) (Figure 4B, 4C). Furthermore XPO1 knockdown decreased CD107a expression on KIR2DS2+ primary NK cells as compared to KIR2DS2- NK cells (Figure 4D, 4E). Thus, endogenously expressed XPO1 is recognized specifically by KIR2DS2+ NK cells.

KIR2DS2-targeted vaccination generates an anti-tumor NK cell response

The activity of NK cells from C*0102-IVDL-vaccinated KIR-Tg mice were tested against 721.221 cells. This demonstrated augmented reactivity against the NAPLVHATL-expressing 72.221 cells as compared to C*0102 expressing cell lines ($p<0.05$) (Figure 5A). Additionally, degranulation of NK cells from C*0102-IVDL-vaccinated mice was greater than that of control vaccinated mice to Huh7 targets ($p<0.005$) (Figure 5B). Furthermore there was a significant increase expression of IFNγ by KIR2DS2+ versus KIR2DS2- NK cells against Huh7:C*0102

($p<0.05$) but not Huh7 cells (Figure 5C). To test anti-HCC responses *in vivo* we used an adoptive transfer model as the KIR-Tg mouse is not permissive for Huh7 cells. KIR-Tg mice were vaccinated with two doses of the DNA vaccine C*0102-IVDL or the control vaccine weekly, splenic NK cells were then adoptively transferred into immunodeficient NSG mice, which had been inoculated with Huh7-C*0102 cells. We observed a significantly delayed growth of the tumor in mice that received C*0102-IVDL-stimulated NK cells compared to control vaccine concomitant with a marked improvement in survival ($p<0.05$) (Figure 5D, 5E). Thus an NK cell targeting vaccine can generate anti-cancer reactivity.

Discussion

We present a novel strategy to therapeutically target KIR and by identifying a cancer-associated peptide ligand provide a rationale for its use as an immunotherapy. From our peptide elution study we identified only one peptide which had the canonical motif for both KIR2DS2 and HLA-C*0102 binding. This peptide was derived from the XPO1 (exportin-1/CRM1) protein, which is thought to function as the sole nuclear exporter for many different tumor suppressor and growth regulatory proteins including p53, p27, FOXO1, IkB, cyclin B1, cyclin D1 and survivin (38). XPO1 is overexpressed and associated with poor prognosis in multiple cancers including hematological malignancies and difficult to treat cancers such as pancreatic cancer and HCC (41, 43, 47). Inhibition of XPO1 is gaining traction as a cancer therapeutic target following clinical trials, and our data suggest it could also be a target for KIR2DS2-based NK cell therapeutics (40).

Previous work has also shown that KIR2DS2+ NK cells can recognize several different cancer targets *in vitro*, including cell lines derived from prostate, breast and ovarian carcinomas (27). However this recognition was not specific to KIR2DS2 and was beta-2-microglobulin independent, suggesting that there may also be non-peptide:MHC class I ligands for KIR2DS2. Additionally, KIR2DS2+ NK cells appear to have a greater potential to mediate ADCC *in vitro* and *in vivo* (28, 29). Thus, the utility of targeting KIR2DS2 in cancer immunotherapy may extend to combination with antibody based therapeutics.

Our *in vivo* studies demonstrated that KIR2DS2 could be targeted using a peptide:MHC specific approach. We observed activation of both KIR2DS2+ and KIR2DS2- NK cells *in vivo*, but activation was preferential for KIR2DS2+ NK cells and, *in vitro*, peptide specific

recognition of 721.221 targets was only noted for splenocytes from mice vaccinated with IVDLMCHATF. One advantage of NK cell therapeutics is that recognition of cancer targets can occur through multiple receptors. Our data is therefore consistent with a model of activation through one receptor and killing mediated by a different receptor; for instance killing of the B16 melanoma cell line is mediated by NKp46, and hence not MHC class I restricted (48). Additionally, we demonstrate peptide cross reactivity of KIR2DS2, as mice vaccinated with IVDLMCHATF were able to recognize the XPO1 peptide NAPLVHATL, and also the HCV peptide LNPSVAATL, consistent with KIR2DS2 recognizing peptides with an AT motif at the carboxy-terminal -1 and -2 positions. Thus, in order to take our findings to the clinic it is not necessary to identify the ligand on the cancerous cell, or to match for HLA class I as KIR2DS2 may bind other group 1 HLA class I allotypes such as HLA-C*0304 (14, 16). This broad specificity provides an advantage for peptide-based NK cell therapy over T cell pMHC therapeutics which require more precise pMHC matching. Additionally as the strategy provides both the peptide and the MHC class I ligand, then no HLA class I matching is required. As NK cells are involved in the early immune response to viral infections, and KIR2DS2 recognizes peptides derived from a many different viruses, then targeting KIR2DS2 by DNA vaccination may also form part of an anti-viral therapeutic strategy.

In conclusion, our work identifies a novel mechanism that activates NK cells through an activating KIR and provides a rationale for testing peptide:MHC-based NK cell therapy in human cancer.

Materials and Methods

Mice

All mice were bred in a closed research facility under specific pathogen-free in individually ventilated cages. Animal experiments were conducted under UK Home Office Project license P4D9C89E and according to Home Office guidelines were approved by the University of Southampton's ethical committee. KIR transgenic mouse expressing a complete human KIR B haplotype, on a C57BL6 background MHC class I–deficient $Kb^{-/-}$ $Db^{-/-}$ were a kind gift from J Van Bergen (35). For both vaccination and tumor models experiments, mice were aged between 8-14 weeks. Littermates were randomly assigned to experimental groups at the start of the experiment.

DNA vaccination

DNA constructs were made expressing HLA-C*0102 alone or linked with the T2A self-cleaving peptide, and peptide as previously described (14). A control construct IVDLMCHAAA (C*0102-AAA) was also made. DNA was cloned into pIB2 and 50µg of endotoxin free plasmid DNA in 50ul of PBS used to inject KIR-Tg mice intramuscularly.

Tumor models

For the melanoma model, KIR-Tg mice were subcutaneously injected with $2.5x10^5$ B16F10 cells into the mice left flank in 100ul PBS at day 0 and subsequently injected intramuscularly with 50ug of endotoxin-free DNA plasmid in 50ul PBS at days 0 and 7. For the adoptive transfer model, $1x10^6$ purified NK cells from 2 weeks vaccinated KIR-Tg mice spleen were injected intravenously via the tail vein into NOD.*Cg-Prkdc*^{scid}*Il2rg*^{tm1Wjl}/SzJ (NSG™) mice. NSG mice were injected with $2x10^6$ Huh7:C*0102 cells subcutaneously into the flank in 100ul PBS on day 0 and received purified NK cells from KIR-Tg mice at day 0 and 14. Mice were monitored for palpable tumors on alternate days, and tumor growth was monitored by measuring the length and width using calipers. Mice were culled at the humane endpoint.

Murine Cell isolation

Single cell suspensions were prepared from spleens and livers. Organs isolated were cut into small pieces, mechanically dissociated and put through a 70 µm cell strainer. The liver single cell suspension was resuspended in 33% Percoll and centrifuged for 20 min at 2000 rpm at room temperature. Cells were recovered, red blood cells were eliminated using ammonium-chloride-potassium (ACK) lysis buffer and cells were washed twice in PBS. For the adoptive transfer, NK cells were purified from 2 weeks-DNA vaccinated KIR-Tg mice splenocytes using MACS technology (Miltenyi Biotec, NK cell isolation kit II). Purity was > 80% with < 3% $CD3^+$ T cells.

Cell lines

HLA class I-deficient 721.221 lymphoblastoid EBV-B cells were cultured in R10 medium (RPMI 1640 supplemented with 1% penicillin-streptomycin (Life Technologies) and 10% heat inactivated fetal bovine serum (FBS; Sigma). 721.221 cells were transduced with the pIB2 constructs to express HLA-C*0102 alone or together with peptides LNPSVAATL, IVDLMCHATF or NAPLVHATL and maintained in R10 medium selected with blasticidin. B16F10 cells were cultured in Dulbecco's modified Eagle's medium (DMEM) with 1% penicillin-streptomycin (Life Technologies) and 10% FBS.

Flow cytometry staining of murine cells

Single-cell suspensions were incubated with 2.4G2 mAb (BD Biosciences) for 10 min on ice to block Fc receptors. Cells were then surface stained for 30 min at 4C before washed for analysis. Antibodies used were anti-mouse CD3ε-PE, NK1.1-BV421, CD11b-APC-Cy5, CD27-BV510, KLRG1-PECy7, (Biolegend). The 1F12-FITC antibody was used to selectively stain KIR2DS2 (49). Events were acquired on Aria II (BD Biosciences) using the FACSDiva software (BD Biosciences) and analyzed with FlowJo software (Treestar).

CD107a and IFN-γ secretion assays from murine splenocytes

Freshly isolated splenocytes were cultured with different target cells for 5h at an E:T ratio of 5:1 or 10:1 with anti-CD107a AF647 (Biolegend) and Golgi stop (BD Biosciences) for the last 4h. The cells were stained with 1F12-FITC, CD3-PE, NK1.1-BV421 (Biolegend). For the IFN-γ secretion assay, splenocytes were cultured with target cells at an E:T ratio of 5:1 or 10:1 for 22h, with Golgi stop (BD Biosciences) for the last 4h. Splenocytes were surface stained with 1F12-FITC, CD3-PE, NK1.1-BV421 antibodies. Cells were fixed for 20 min at 4°C and permeabilized with anti-mouse IFNγ-APC (Biolegend) for 15 min at 4°C (BD Cytofix/Cytoperm buffers)

RNA Seq data analysis and processing

RNA was isolated using the RNeasy Kit (QIAGEN) according to the manufacturer's instructions. The library preparation was done using the QIAseq UPX 3' Transcriptome Kit (QIAGEN). A total of 10ng purified RNA was converted into cDNA NGS libraries. During reverse transcription, each cell is tagged with a unique ID (up to 384 different IDs) and each RNA molecule is tagged with a unique molecular index (UMI). Then RNA was converted to cDNA. The cDNA was amplified using PCR and during the PCR indices were added. The library pool was then sequenced on a NextSeq500 sequencing instrument according to the manufacturer's instructions. Raw data was de-multiplexed and FASTQ files for each sample were generated using the bcl2fastq software (Illumina inc.). FASTQ data were checked using the FastQC tool (https://www.bioinformatics.babraham.ac.uk/projects/fastqc/)

Differential Gene Expression analysis

For differential gene expression analysis raw counts from RNA-Seq were processed in Bioconductor package EdgeR(50) variance was estimated and size factor normalized using TMM. Genes with minimum 4 reads at minimum 40% samples were included in the downstream analyses. Differentially expressed genes (DEG) were identified applying significance threshold FDR $p<0.05$.

Hierarchical clustering and principal component analysis

Blind, normalized log2 values calculated by EdgeR were used for principal component analysis and to calculate Euclidean distances for hierarchical clustering using Ward's method. For heatmaps in Fig.. 5b these normalized log2 values of all high-fold change peaks were used to hierarchically cluster peak regions into seven clusters, with the top 100 most variable genes (based on calculated variance across all samples).

Gene ontology and pathway enrichment analysis

Gene ontology and pathway enrichment analysis were done using CAMERA (51), Ensemble of Gene Set Enrichment Analyses (EGSEA) (52) and ToppGene (53) on-line tool. All analyses used default settings considering mouse orthologs from the MSigDB v5.2 databases retrieved from http://bioinf.wehi.edu.au/software/MSigDB/. Only pathway terms with a minimum of 25 genes were considered and used for multiple-hypothesis correction. Enriched pathways were filtered for those that showed Padj < 0.05 for both P values as calculated for the contrast C*0102-IVDL vs C*0102-AAA in KIR2DS+ and KIR2DS2- NK cell populations. Pathway results were further filtered on those that showed the lowest p.adj values.

Peptide elution, identification and quantification

Isolation of peptides bound to HLA class I molecules

HLA class I peptides were eluted from Huh7 and Huh7:HLA-C*0102 cells essentially as described before (54-56). In brief, cells were lysed in 0.5% IGEPAL, 50 mM Tris-HCl pH 8.0, 150 mM NaCl supplemented with protease inhibitors (Complete Protease Inhibitor Cocktail Tablet; Roche Molecular Biochemicals) for 45 min at 4 °C. Lysates were cleared by ultracentrifugation at 40.000g and HLA class I complexes were immunoaffinity purified using DT9 (HLA-C-specific) and W6/32 (pan anti-HLA-A, B, C) monoclonal antibodies bound to protein A sepharose (GE Healthcare).

Fractionation of HLA-bound peptides by reverse-phase high-performance liquid chromatography (RP-HPLC)

The HLA-peptide eluates were loaded onto a 4.6 mm internal diameter x 50 mm monolithic C18 RP-HPLC column (Chromolith Speed Rod; Merck) at a flow rate of 1 ml/min using an EttanLC HPLC system (GE Healthcare) with buffer A (0.1% trifluoroacetic acid (TFA)) and buffer B (80% ACN / 0.1% TFA) as mobile phases. The bound peptides were separated from the class I heavy chains and ß2m molecules using increasing concentration of buffer B. Peptide-containing fractions were collected, vacuum concentrated to ~5 µl and reconstituted to 15 µl with 0.1% formic acid (FA). Indexed retention time (iRT) peptides (Escher et al., 2012) were spiked in for retention time alignment.

Identification of HLA bound-peptides using data-dependent acquisition (DDA)

Using a Dionex UltiMate 3000 RSLCnano system equipped with a Dionex UltiMate 3000 RS autosampler, peptides were loaded via an Acclaim PepMap 100 trap column (100 µm x 2 cm, nanoViper, C18, 5 µm, 100Å; Thermo Scientific) onto an Acclaim PepMap RSLC analytical column (75 µm x 50 cm, nanoViper, C18, 2 µm, 100Å; Thermo Scientific). The peptides were separated by increasing concentrations of 80% ACN / 0.1% FA at a flow rate of 250 nl/min for 95 min and analyzed with a QExactive mass spectrometer (Thermo Scientific). In each cycle, a full ms1 scan (resolution: 70.000; AGC target: 3e6; maximum IT: 50 ms; scan range: 375-1600 m/z) preceded up to 12 subsequent ms2 scans (resolution: 17.500; AGC target: 2e5; maximum IT: 110 ms; isolation window: 1.8 m/z; scan range: 200-2000 m/z; NCE: 27). To minimize repeated sequencing of the same peptides, the dynamic exclusion was set to 15 sec and the 'exclude isotopes' option was activated.

Quantification of HLA bound-peptides using data-independent acquisition (DIA)

An Orbitrap Fusion Tribrid mass spectrometer (Thermo Scientific) coupled to an identical LC setup as described above (Dionex UltiMate 3000 LC system) has been used to quantify HLA-

bound peptides using data-independent acquisition (DIA). 50 sequential DIA windows with an isolation width of 12 m/z between 375 - 975 m/z have been acquired in 2 consecutive injections (resolution: 30.000; AGC target: 1e6; maximum IT: 54 ms; Collision energy: 32%; scan range: 200-2000 m/z) following a full ms1 scan (resolution: 120.000; AGC target: 4e5; maximum IT: 50 ms; scan range: 375-1575 m/z). A 155 min gradient of increasing concentrations of 80% ACN / 0.1% FA has been used to separate the peptides for the DIA acquisition.

Data analysis

Acquired DDA .raw files were searched against the human UniProtKB/SwissProt database (v2012_07) using Byonic (Protein Metrics) embedded in Proteome Discoverer (Thermo Scientific) to obtain peptide sequence information. Only peptides identified at a false discovery rate (FDR) of 1% based on a decoy database were considered for further analysis. Spectronaut Orion (Biognosys) was used to create the corresponding spectral library as well as to evaluate all DIA data using in-house, peptide-centric parameters.

KIR2DS2 tetramer staining

Fluorescently labelled tetramers containing PE-conjugated streptavidin and biotinylated KIR2DS2 molecules were used as previously described (14). Data was acquired on a BD FACS Accuri and analyzed using C6 software.

Degranulation and cytotoxicity assays

PBMC were obtained with full ethical approval from the National Research Ethics Committee (NREC) reference 06/Q1701/120. For degranulation assays, PBMCs were stimulated overnight with IL-15 (1ng/ml) and co-incubated with 721.221 or Huh7:HLA-C*0102 cells at 10:1, 5:1 or 2.5:1 as indicated for 4 hours with anti-CD107a-AF647. Golgistop was added 1 hour after co-incubation and cells were then stained and analyzed by flow cytometry on a BD FACS Aria. Data was analyzed by FlowJo software. For Huh7:HLA-C*0102 cytotoxicity assays, cells were detected based on expression of GFP encoded within the HLA-C*0102

construct. Target cells were co-incubated with the indicated NK cell population for 4 hours. Cells were then stained with LIVE/DEAD stain for 30 minutes and analyzed by flow cytometry, gating on the target cell population. Percentage cytotoxicity was calculated as LIVE/DEAD-positive cells in the presence of indicated effector cells minus LIVE/DEAD-positive cells in the absence of effector cells. For XPO1 knockdown, Huh7:HLA-C*0102 cells were transfected using Jetprime (Polyplus, UK) reagent with siRNA control or siRNA targeting XP01 (ThermoFisherScientific). XP01 protein expression was analyzed by immunoblotting after 48 hours and cells were used in cytotoxicity and degranulation assays 48 hours post transfection.

Immunoblotting

NKL-KIR2DS2 or NKL-KIR2DL2 were co-incubated with 721.221:HLA-C*0102 or 721.221:HLA-C*0102+NAPLVHATL cells as indicated for 5min at an E:T ratio of 1:1. Cells were then lysed in NP40 Cell Lysis Buffer (Fisher Scientific UK Ltd) and analyzed by immunoblotting. Antibodies recognizing phospho-VAV1, VAV1 and actin were used with HRP-conjugated antibodies and visualized using ChemiDoc-It Imaging system with VisionWorks software. Bands were quantified using ImageJ software.

Statistical analysis

Experimental statistical analyses were performed using Graph-Pad Prism 7.0 software. Student two-tailed t test was used for comparison between two groups and two-way ANOVA with post-hoc analysis were used to compare more than two groups. Data were considered statistically significant at $p < 0.05$. For the tumor model statistical comparisons between survival to the humane end point was performed by Log-rank test (Mantel-cox).

Author contribution: SIK, PR, MDB, BM, RBS designed experiments; PR, MDB, BM, RF RBS, LBL, RA performed experiments; AVP, PR, MDB, RBS and SIK analyzed data; CR provided key reagents; SIK, AA-S, AWP, MP supervised experiments and interpreted data; PR, MDB, RBS, AVP, AA-S and SIK wrote the manuscript.

Acknowledgements: We would like to than Jeroen van Bergen and John Trowsdale for KIR-Tg mice and Mohammed Naiyer for technical assistance.

Funding: The work was funded by grants M019829 and S009338 from the MRC UK and grant 19917 from CRUK.

References

1. Demaria O, Cornen S, Daeron M, Morel Y, Medzhitov R, and Vivier E. Harnessing innate immunity in cancer therapy. *Nature.* 2019;574(7776):45-56.
2. Cooley S, Parham P, and Miller JS. Strategies to activate NK cells to prevent relapse and induce remission following hematopoietic stem cell transplantation. *Blood.* 2018;131(10):1053-62.
3. Hu W, Wang G, Huang D, Sui M, and Xu Y. Cancer Immunotherapy Based on Natural Killer Cells: Current Progress and New Opportunities. *Front Immunol.* 2019;10:1205.
4. Vilches C, and Parham P. KIR: diverse, rapidly evolving receptors of innate and adaptive immunity. *Annu Rev Immunol.* 2002;20:217-51.
5. Leone P, De Re V, Vacca A, Dammacco F, and Racanelli V. Cancer treatment and the KIR-HLA system: an overview. *Clin Exp Med.* 2017;17(4):419-29.
6. Bao X, Hanson AL, Madeleine MM, Wang SS, Schwartz SM, Newell F, et al. HLA and KIR Associations of Cervical Neoplasia. *J Infect Dis.* 2018;218(12):2006-15.
7. Cariani E, Pilli M, Zerbini A, Rota C, Olivani A, Zanelli P, et al. HLA and killer immunoglobulin-like receptor genes as outcome predictors of hepatitis C virus-related hepatocellular carcinoma. *Clin Cancer Res.* 2013;19(19):5465-73.
8. Carrington M, Wang S, Martin MP, Gao X, Schiffman M, Cheng J, et al. Hierarchy of resistance to cervical neoplasia mediated by combinations of killer immunoglobulin-like receptor and human leukocyte antigen loci. *J Exp Med.* 2005;201(7):1069-75.
9. Cornillet M, Jansson H, Schaffer M, Hertwig L, Berglin L, Zimmer CL, et al. Imbalance of Genes Encoding Natural Killer Immunoglobulin-Like Receptors and Human Leukocyte Antigen in Patients With Biliary Cancer. *Gastroenterology.* 2019;157(4):1067-80 e9.

10. Impola U, Turpeinen H, Alakulppi N, Linjama T, Volin L, Niittyvuopio R, et al. Donor Haplotype B of NK KIR Receptor Reduces the Relapse Risk in HLA-Identical Sibling Hematopoietic Stem Cell Transplantation of AML Patients. *Front Immunol.* 2014;5:405.

11. Almalte Z, Samarani S, Iannello A, Debbeche O, Duval M, Infante-Rivard C, et al. Novel associations between activating killer-cell immunoglobulin-like receptor genes and childhood leukemia. *Blood.* 2011;118(5):1323-8.

12. Vey N, Karlin L, Sadot-Lebouvier S, Broussais F, Berton-Rigaud D, Rey J, et al. A phase 1 study of lirilumab (antibody against killer immunoglobulin-like receptor antibody KIR2D; IPH2102) in patients with solid tumors and hematologic malignancies. *Oncotarget.* 2018;9(25):17675-88.

13. Stewart CA, Laugier-Anfossi F, Vely F, Saulquin X, Riedmuller J, Tisserant A, et al. Recognition of peptide-MHC class I complexes by activating killer immunoglobulin-like receptors. *Proc Natl Acad Sci U S A.* 2005;102(37):13224-9.

14. Naiyer MM, Cassidy SA, Magri A, Cowton V, Chen K, Mansour S, et al. KIR2DS2 recognizes conserved peptides derived from viral helicases in the context of HLA-C. *Sci Immunol.* 2017;2(15).

15. Sim MJW, Rajagopalan S, Altmann DM, Boyton RJ, Sun PD, and Long EO. Human NK cell receptor KIR2DS4 detects a conserved bacterial epitope presented by HLA-C. *Proc Natl Acad Sci U S A.* 2019;116(26):12964-73.

16. David G, Djaoud Z, Willem C, Legrand N, Rettman P, Gagne K, et al. Large spectrum of HLA-C recognition by killer Ig-like receptor (KIR)2DL2 and KIR2DL3 and restricted C1 SPECIFICITY of KIR2DS2: dominant impact of KIR2DL2/KIR2DS2 on KIR2D NK cell repertoire formation. *J Immunol.* 2013;191(9):4778-88.

17. Boyington JC, Brooks AG, and Sun PD. Structure of killer cell immunoglobulin-like receptors and their recognition of the class I MHC molecules. *Immunol Rev.* 2001;181:66-78.

18. Das J, and Khakoo SI. NK cells: tuned by peptide? *Immunol Rev.* 2015;267(1):214-27.

19. Blunt MD, Rettman P, Bastidas-Legarda LY, Fulton R, Capizzuto V, Naiyer MM, et al. A novel antibody combination to identify KIR2DS2(high) natural killer cells in KIR2DL3/L2/S2 heterozygous donors. *HLA.* 2019;93(1):32-5.

20. Cooley S, Trachtenberg E, Bergemann TL, Saeteurn K, Klein J, Le CT, et al. Donors with group B KIR haplotypes improve relapse-free survival after unrelated hematopoietic cell transplantation for acute myelogenous leukemia. *Blood.* 2009;113(3):726-32.

21. Cooley S, Weisdorf DJ, Guethlein LA, Klein JP, Wang T, Marsh SG, et al. Donor killer cell Ig-like receptor B haplotypes, recipient HLA-C1, and HLA-C mismatch enhance the clinical benefit of unrelated transplantation for acute myelogenous leukemia. *J Immunol.* 2014;192(10):4592-600.

22. Bachanova V, Weisdorf DJ, Wang T, Marsh SGE, Trachtenberg E, Haagenson MD, et al. Donor KIR B Genotype Improves Progression-Free Survival of Non-Hodgkin Lymphoma Patients Receiving Unrelated Donor Transplantation. *Biol Blood Marrow Transplant.* 2016;22(9):1602-7.

23. Sekine T, Marin D, Cao K, Li L, Mehta P, Shaim H, et al. Specific combinations of donor and recipient KIR-HLA genotypes predict for large differences in outcome after cord blood transplantation. *Blood.* 2016;128(2):297-312.

24. Alomar SY, Alkhuriji A, Trayhyrn P, Alhetheel A, Al-Jurayyan A, and Mansour L. Association of the genetic diversity of killer cell immunoglobulin-like receptor genes

and HLA-C ligand in Saudi women with breast cancer. *Immunogenetics.* 2017;69(2):69-76.

25. Beksac K, Beksac M, Dalva K, Karaagaoglu E, and Tirnaksiz MB. Impact of "Killer Immunoglobulin-Like Receptor /Ligand" Genotypes on Outcome following Surgery among Patients with Colorectal Cancer: Activating KIRs Are Associated with Long-Term Disease Free Survival. *PLoS One.* 2015;10(7):e0132526.

26. Wisniewski A, Jankowska R, Passowicz-Muszynska E, Wisniewska E, Majorczyk E, Nowak I, et al. KIR2DL2/S2 and HLA-C C1C1 genotype is associated with better response to treatment and prolonged survival of patients with non-small cell lung cancer in a Polish Caucasian population. *Hum Immunol.* 2012;73(9):927-31.

27. Thiruchelvam-Kyle L, Hoelsbrekken SE, Saether PC, Bjornsen EG, Pende D, Fossum S, et al. The Activating Human NK Cell Receptor KIR2DS2 Recognizes a beta2-Microglobulin-Independent Ligand on Cancer Cells. *J Immunol.* 2017;198(7):2556-67.

28. Gras Navarro A, Kmiecik J, Leiss L, Zelkowski M, Engelsen A, Bruserud O, et al. NK cells with KIR2DS2 immunogenotype have a functional activation advantage to efficiently kill glioblastoma and prolong animal survival. *J Immunol.* 2014;193(12):6192-206.

29. Siebert N, Jensen C, Troschke-Meurer S, Zumpe M, Juttner M, Ehlert K, et al. Neuroblastoma patients with high-affinity FCGR2A, -3A and stimulatory KIR 2DS2 treated by long-term infusion of anti-GD2 antibody ch14.18/CHO show higher ADCC levels and improved event-free survival. *Oncoimmunology.* 2016;5(11):e1235108.

30. Rezvani K. Adoptive cell therapy using engineered natural killer cells. *Bone Marrow Transplant.* 2019;54(Suppl 2):785-8.

31. Felices M, Kodal B, Hinderlie P, Kaminski MF, Cooley S, Weisdorf DJ, et al. Novel CD19-targeted TriKE restores NK cell function and proliferative capacity in CLL. *Blood Adv.* 2019;3(6):897-907.

32. Vallera DA, Felices M, McElmurry R, McCullar V, Zhou X, Schmohl JU, et al. IL15 Trispecific Killer Engagers (TriKE) Make Natural Killer Cells Specific to CD33+ Targets While Also Inducing Persistence, In Vivo Expansion, and Enhanced Function. *Clin Cancer Res.* 2016;22(14):3440-50.

33. Andre P, Denis C, Soulas C, Bourbon-Caillet C, Lopez J, Arnoux T, et al. Anti-NKG2A mAb Is a Checkpoint Inhibitor that Promotes Anti-tumor Immunity by Unleashing Both T and NK Cells. *Cell.* 2018;175(7):1731-43 e13.

34. Ott PA, Hu Z, Keskin DB, Shukla SA, Sun J, Bozym DJ, et al. An immunogenic personal neoantigen vaccine for patients with melanoma. *Nature.* 2017;547(7662):217-21.

35. van Bergen J, Thompson A, van Pel M, Retiere C, Salvatori D, Raulet DH, et al. HLA reduces killer cell Ig-like receptor expression level and frequency in a humanized mouse model. *J Immunol.* 2013;190(6):2880-5.

36. Rich NE, Hester C, Odewole M, Murphy CC, Parikh ND, Marrero JA, et al. Racial and Ethnic Differences in Presentation and Outcomes of Hepatocellular Carcinoma. *Clin Gastroenterol Hepatol.* 2019;17(3):551-9 e1.

37. Kurokohchi K, Carrington M, Mann DL, Simonis TB, Alexander-Miller MA, Feinstone SM, et al. Expression of HLA class I molecules and the transporter associated with antigen processing in hepatocellular carcinoma. *Hepatology.* 1996;23(5):1181-8.

38. Zheng Y, Gery S, Sun H, Shacham S, Kauffman M, and Koeffler HP. KPT-330 inhibitor of XPO1-mediated nuclear export has anti-proliferative activity in hepatocellular carcinoma. *Cancer Chemother Pharmacol.* 2014;74(3):487-95.

39. Kim J, McMillan E, Kim HS, Venkateswaran N, Makkar G, Rodriguez-Canales J, et al. XPO1-dependent nuclear export is a druggable vulnerability in KRAS-mutant lung cancer. *Nature.* 2016;538(7623):114-7.

40. Chari A, Vogl DT, Gavriatopoulou M, Nooka AK, Yee AJ, Huff CA, et al. Oral Selinexor-Dexamethasone for Triple-Class Refractory Multiple Myeloma. *N Engl J Med.* 2019;381(8):727-38.

41. Birnbaum DJ, Finetti P, Birnbaum D, Mamessier E, and Bertucci F. XPO1 Expression Is a Poor-Prognosis Marker in Pancreatic Adenocarcinoma. *J Clin Med.* 2019;8(5).

42. Camus V, Miloudi H, Taly A, Sola B, and Jardin F. XPO1 in B cell hematological malignancies: from recurrent somatic mutations to targeted therapy. *J Hematol Oncol.* 2017;10(1):47.

43. Chen L, Huang Y, Zhou L, Lian Y, Wang J, Chen D, et al. Prognostic roles of the transcriptional expression of exportins in hepatocellular carcinoma. *Biosci Rep.* 2019;39(8).

44. Di Marco M, Schuster H, Backert L, Ghosh M, Rammensee HG, and Stevanovic S. Unveiling the Peptide Motifs of HLA-C and HLA-G from Naturally Presented Peptides and Generation of Binding Prediction Matrices. *J Immunol.* 2017;199(8):2639-51.

45. Hilton HG, McMurtrey CP, Han AS, Djaoud Z, Guethlein LA, Blokhuis JH, et al. The Intergenic Recombinant HLA-B *46:01 Has a Distinctive Peptidome that Includes KIR2DL3 Ligands. *Cell Rep.* 2017;19(7):1394-405.

46. Fadda L, Borhis G, Ahmed P, Cheent K, Pageon SV, Cazaly A, et al. Peptide antagonism as a mechanism for NK cell activation. *Proc Natl Acad Sci U S A.* 2010;107(22):10160-5.

47. Wang AY, and Liu H. The past, present, and future of CRM1/XPO1 inhibitors. *Stem Cell Investig.* 2019;6:6.

48. Glasner A, Ghadially H, Gur C, Stanietsky N, Tsukerman P, Enk J, et al. Recognition and prevention of tumor metastasis by the NK receptor NKp46/NCR1. *J Immunol.* 2012;188(6):2509-15.

49. David G, Morvan M, Gagne K, Kerdudou N, Willem C, Devys A, et al. Discrimination between the main activating and inhibitory killer cell immunoglobulin-like receptor positive natural killer cell subsets using newly characterized monoclonal antibodies. *Immunology.* 2009;128(2):172-84.

50. Robinson MD, McCarthy DJ, and Smyth GK. edgeR: a Bioconductor package for differential expression analysis of digital gene expression data. *Bioinformatics.* 2010;26(1):139-40.

51. Wu D, and Smyth GK. Camera: a competitive gene set test accounting for inter-gene correlation. *Nucleic Acids Res.* 2012;40(17):e133.

52. Alhamdoosh M, Law CW, Tian L, Sheridan JM, Ng M, and Ritchie ME. Easy and efficient ensemble gene set testing with EGSEA. *F1000Res.* 2017;6:2010.

53. Chen J, Bardes EE, Aronow BJ, and Jegga AG. ToppGene Suite for gene list enrichment analysis and candidate gene prioritization. *Nucleic Acids Res.* 2009;37(Web Server issue):W305-11.

54. Croft NP, Smith SA, Wong YC, Tan CT, Dudek NL, Flesch IE, et al. Kinetics of antigen expression and epitope presentation during virus infection. *PLoS Pathog.* 2013;9(1):e1003129.

55. Illing PT, Vivian JP, Dudek NL, Kostenko L, Chen Z, Bharadwaj M, et al. Immune self-reactivity triggered by drug-modified HLA-peptide repertoire. *Nature.* 2012;486(7404):554-8.

56. Schittenhelm RB, Sivaneswaran S, Lim Kam Sian TC, Croft NP, and Purcell AW. Human Leukocyte Antigen (HLA) B27 Allotype-Specific Binding and Candidate

Arthritogenic Peptides Revealed through Heuristic Clustering of Data-independent Acquisition Mass Spectrometry (DIA-MS) Data. *Mol Cell Proteomics.* 2016;15(6):1867-76.

FIGURE 1

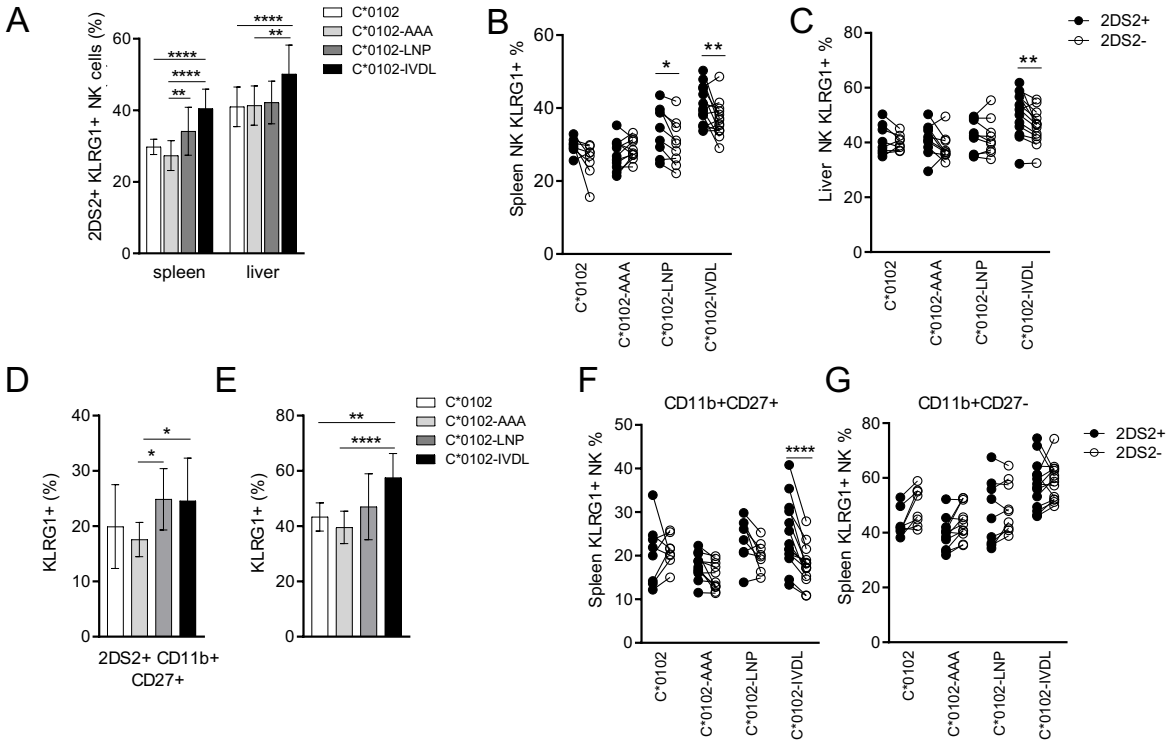

Fig. 1: A pepetide:MHC DNA vaccine that targets KIR2DS2 activates NK cells

KIR-Tg mice were injected intramuscularly using two doses of the indicated DNA construct one week apart and then assessed for activation of NK cells by flow cytometry for expression of KLRG1. **A)** The frequency of KLRG1 expression on KIR2DS2+ NK cells in the spleen and livers of KIR-Tg mice vaccinated with DNA plasmids containing HLA-C*0102 (C*0102, white bars), HLA-C*0102 plus IVDLMCHATAAA (C*0102-AAA, light gray bars), HLA-C*0102-LNPSVAATL (C*0102-LNP, dark gray bars), HLA-C*0102-IVDLMCHATF (C*0102-IVDL, black bars). **B, C)** Comparison of KLRG1 frequencies on KIR2DS2+ (filled circles) or KIR2DS2- (open circles) CD3-NK1.1+ NK cells in the spleens (**B**) and livers (**C**) following vaccination. **D, E)** KLRG1 on splenic CD11b+CD27+ (**D**) and CD11b+CD27- (**E**) NK cell sub-populations following vaccination. **F,G)** Comparison of KLRG1 expression on KIR2DS2+ and KIR2DS2- splenic NK cells in the CD11b+CD27+ (**F**) and CD11b+CD27- (**G**) sub-populations. N=8-14 mice per group. For all plots comparisons between two groups

were made by paired t test (2 groups) and 2-way ANOVA (more than 2 groups) (*$p < 0.05$, **$p < 0.01$, ****$p < 0.001$).

FIGURE 2

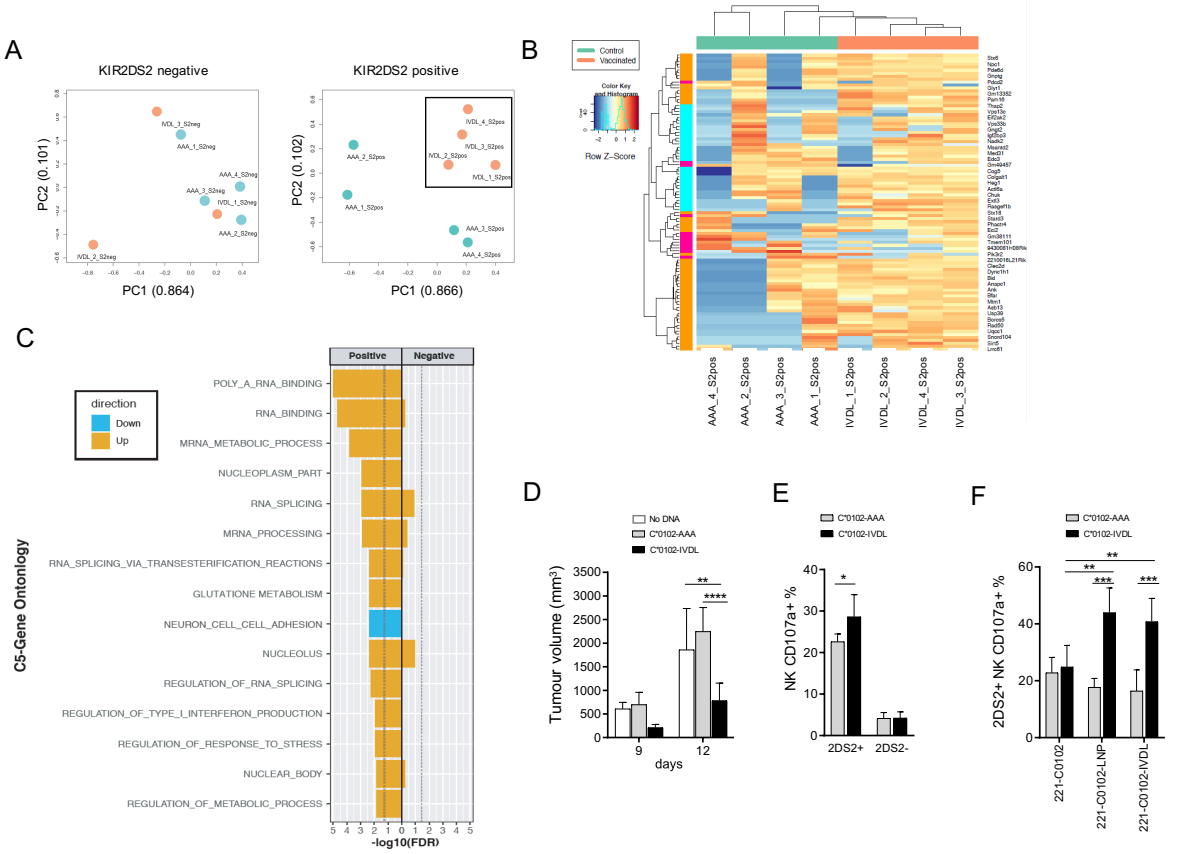

Fig. 2: Preferential activation of KIR2DS2 NK cells by peptide-based DNA vaccination

A) Principal component analysis (PCA) of whole NK cell transcriptomes from C*0102-IVDL and C*0102-AAA vaccinated mice. KIR2DS2+ NK cells from both groups are shown in the left panel and KIR2DS2-positive NK cells in the right panel. Counts were normalized and filtered using EdgeR. The first two components of the PCA are shown. **B)** Heatmap of the top 100 differentially expressed genes derived from the comparison of KIR2DS2 positive NK cells from C*0102-IVDL and C*0102-AAA vaccinated mice. **C)** EGSEA analysis of C5 signatures (GO) comparing KIR2DS2+ and KIR2DS2- NK cell populations in both C*0102-IVDL and control vaccinated mice. Effect significances were calculated individually for each arm of the study and the plot indicates the overall effects of vaccination on KIR2DS2+ NK

cells in the C*0102-IVDL vaccinated mice ("positive") as compared to the other three groups ("negative"). The color denotes the direction of the change and the size of the bar represents the -Log10(FDR). All categories shown were significant at FDR<0.05. **D)** KIR-Tg mice were injected subcutaneously with B16F10 melanoma cells on day 0 and then vaccinated intramuscularly with C*0102-IVDL (black bars) or C*0102-AAA (gray bars) on days 0 and 7 or untreated (white bars) and tumor volume measured. (n=4 mice per group). **E**,**F)** Mice were injected intramuscularly with C*0102-IVDL (black bars) or C*0102-AAA (gray bars) on days 0 and day 7 and then NK cells purified from the spleens on day 14 for *in vitro* assays of activation. **E)** shows degranulation of KIR-Tg NK cells to B16F10 melanoma cells (n=4 mice per group). **F**) shows degranulation of KIR2DS2+ KIR-Tg NK cells to human 721.221 cells expressing HLA-C*0102 alone (221-C*0102) or HLA-C*0102 in combination with the peptide: LNPSVAATL (221-C*0102-LNP) or IVDLMCHATF (221-C*0102-IVDL), (n=8 mice per group). Comparisons were by Students t-test (2 groups) or two-way ANOVA (more than 2 groups). For all plots *p < 0.05, **p< 0.01, ***p< 0.005, ****p< 0.001.

FIGURE 3

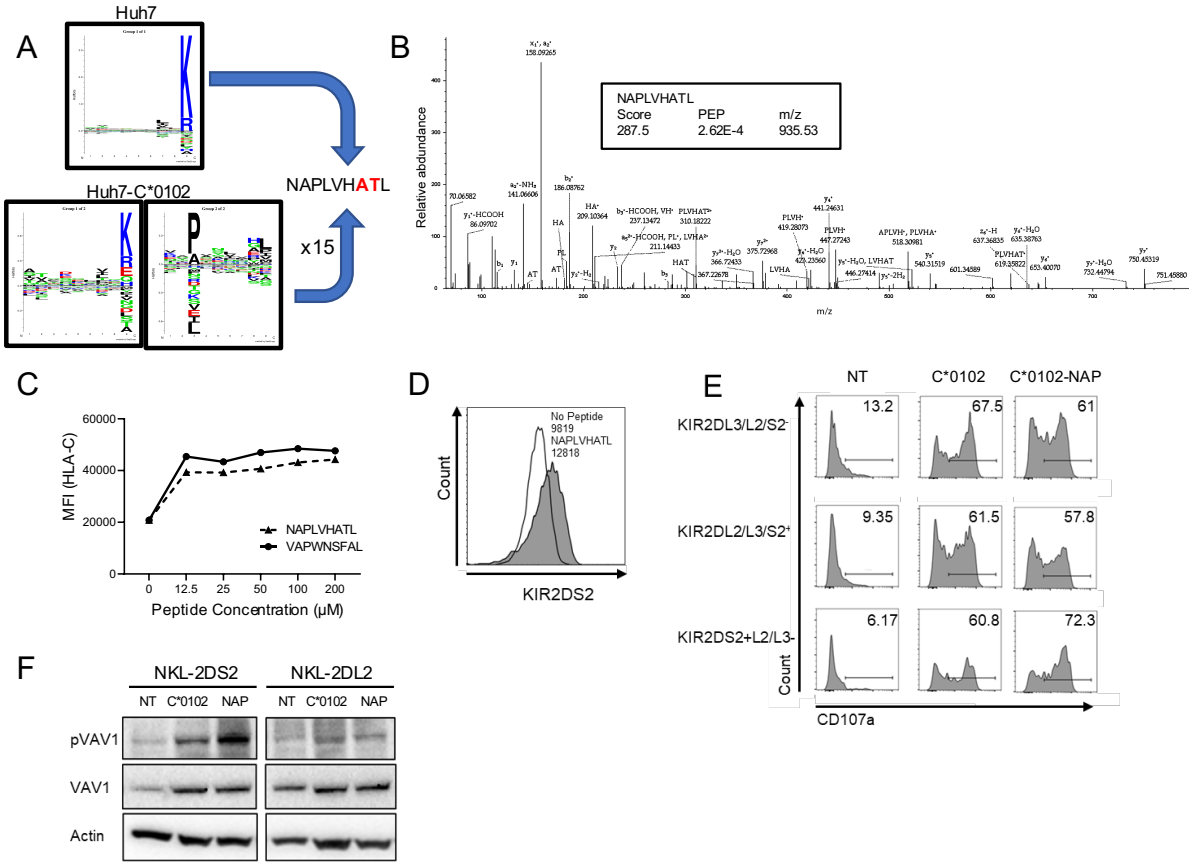

Fig. 3. An XPO1 derived peptide is a ligand for KIR2DS2

A) SeqLogo plots of peptides eluted from Huh7 and Huh7:HLA-C*0102 cell lines. **B)** Representative and annotated ms2 spectrum that has been assigned to the peptide sequence NAPLVHATL. The resulting Byonic score, the posterior error probability (PEP) and the m/z value of the singly protonated species is shown in the inset. **C)** 721.174 cells were incubated with NAPLVHATL at the indicated concentrations, stained for HLA-C using the DT9 antibody and analyzed by flow cytometry. The mean fluorescence intensity (MFI) of DT9 staining compared to the control VAPWNSFAL peptide is shown. **D)** 721.174 were incubated with NAPLVHATL (100µM) and stained with a KIR2DS2-tetramer and analyzed by flow cytometry. Histogram plots of KIR2DS2-staining compared to a no peptide control are shown with MFIs indicated. **E)** 721.221 cells were transfected with HLA-C*0102 alone (C*0102) or in combination with the peptide NAPLVHATL (C*0102-NAP), and the cell lines used as

targets for degranulation assays for IL-15 activated NK cells. CD107a expression on the indicated sub-populations of CD3-CD56+ NK cells was assessed by flow cytometry against these targets (NT, no target). For the gating strategy see Supplementary Figure 5. One representative flow cytometry plots of CD107a expression is shown from six donors tested. **F)** NKL-2DS2 or NKL-2DL2 cells were incubated with either no target (NT), 721.221:HLA-C*0102 (C*0102) or 721.221:HLA-C*0102+NAPLVHATL (NAP) cells for 5 minutes and assessed for VAV1 (Tyr174) phosphorylation by immunoblotting. A representative image from six experiments is shown.

FIGURE 4

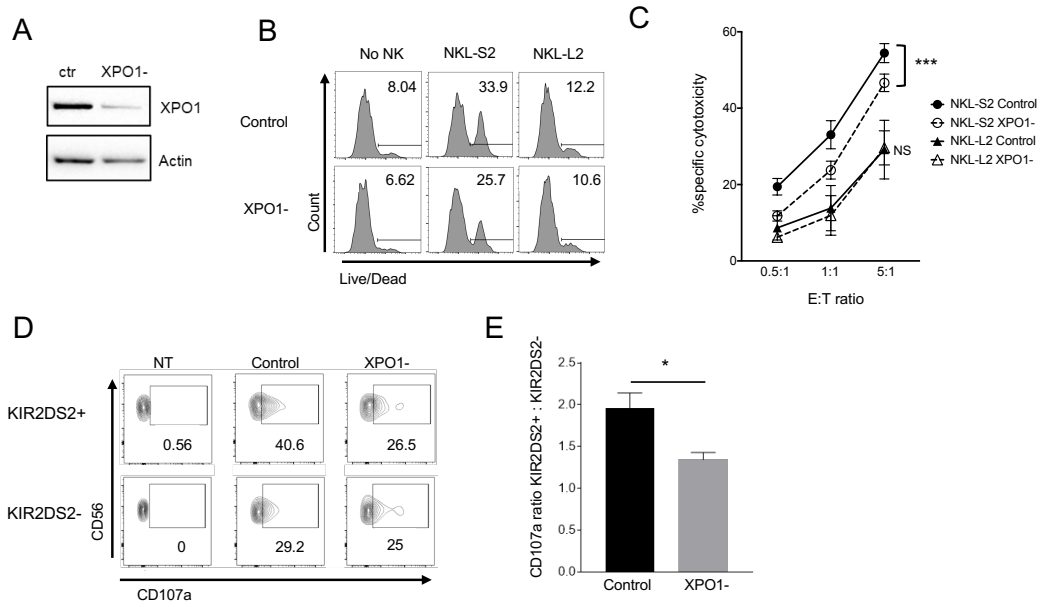

Fig. 4. Silencing of XPO1 expression in Huh7:HLA-C*0102 cells reduces KIR2DS2+ but not KIR2DS2- NK cell activation.

A) Representative immunoblot of XPO1 silencing following XPO1-targeting siRNA treatment of Huh7:HLA-C*0102 cells. **B)** and **C)** Huh7:HLA-C*0102 cells were treated with control or XPO1 targeting siRNA and used as targets in cytotoxicity assays with NKL-S2 or NKL-L2 cells. Killing was determined using the LIVE/DEAD™ stain. Representative plots at an effector:target ratio of 5:1 are shown in **B)** and the mean specific cytotoxicity and SEM from five independent experiments are shown **C)**, (***$p<0.005$)**.** **D)** and **E)** Huh7:HLA-C*0102 cells were treated with control or XPO1-targeting siRNA and used as targets for KIR2DS2+ NK cells in CD107a degranulation assays. CD107a expression in KIR2DS2+ or KIR2DS2- CD3-CD56+ NK cells determined using the 1F12 antibody in KIR2DL2/S2 homozygous

donors was analyzed by flow cytometry. Representative contour plots are shown in **D)** and the ratio of CD107a positivity in KIR2DS2+ to KIR2DS2- NK cells from three donors is shown **E)** (*$p<0.05$).

FIGURE 5

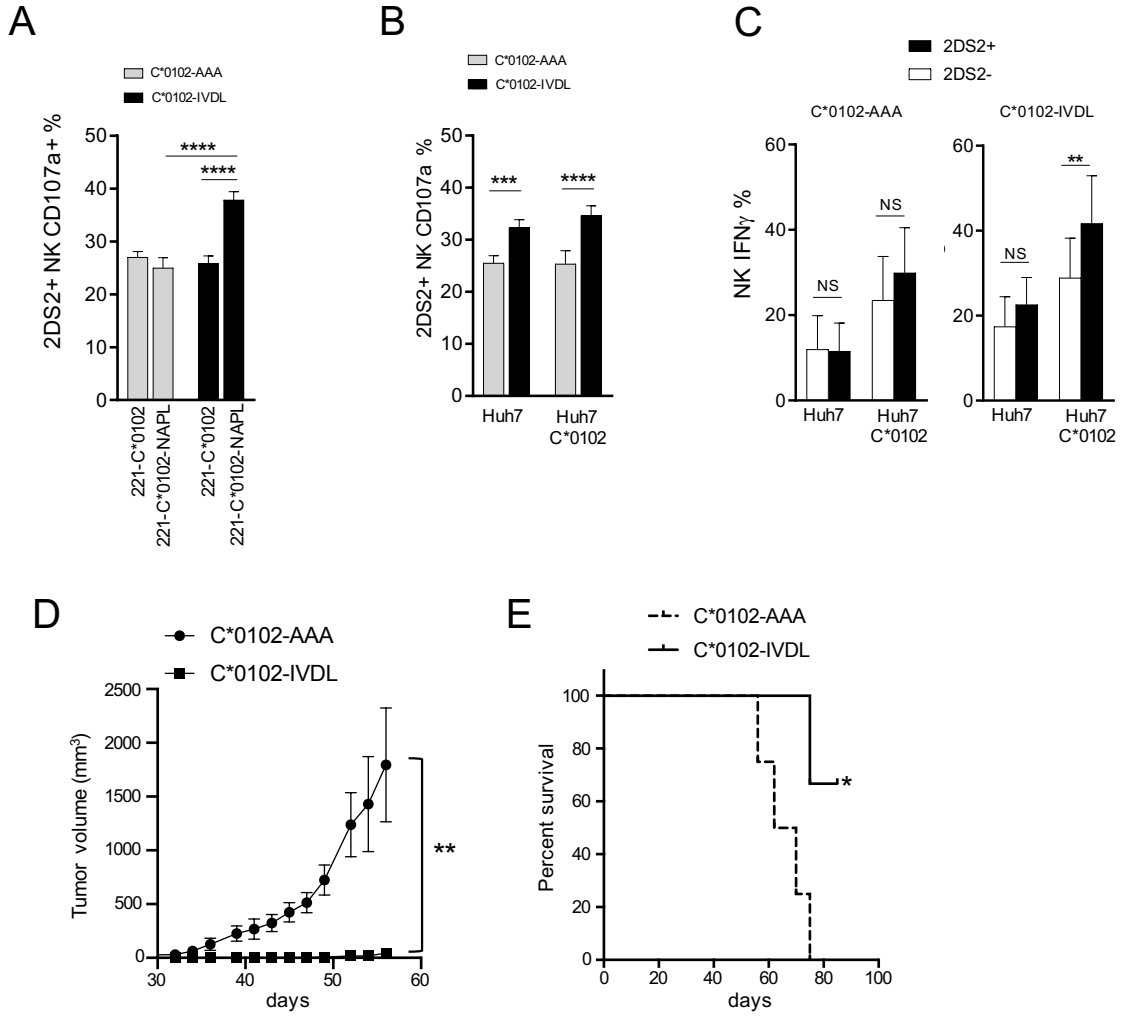

Fig. 5: A peptide:MHC DNA vaccination induces anti-Huh7 NK cell responses

Mice were injected intramuscularly with C*0102-IVDL (black bars) or C*0102-AAA (gray bars on days 0 and day 7 and then NK cells purified from the spleens on day 14 for *in vitro* assays of activation against human target cell lines. **A**) shows degranulation of KIR2DS2+ KIR-Tg NK cells to 721.221:HLA-C*0102+NAPLVHATL targets (n=4 mice per group) and **B)** to Huh7 and Huh7:C*0102 targets (n=4 mice per group). **C)** shows expression of IFNγ on KIR2DS2+ or KIR2DS2- NK cells following culture with Huh7 or Huh7:C*0102 targets (n=8 mice per group). **D, E)** NK cells from KIR-Tg mice vaccinated either with C*0102-IVDL or

C*0102-AAA. as a peptide control, were adoptively transferred into NSG mice inoculated subcutaneously with Huh7:C*0102 hepatoma cells. Tumour volume was measured (**D**) and survival to a humane endpoint determined (**E**) (n=4 mice per group). For all plots *$p < 0.05$, **$p < 0.01$, ***$p < 0.005$, ****$p < 0.001$, by paired t test between 2 groups and 2-way ANOVA for more than 2 groups.